

STRUCTURAL AND MAGNETIC PROPERTIES OF CAST IRON FOR CYCLOTRONS

S. Zaremba, E. Forton, IBA, Louvain-la-Neuve, Belgium

E. Ferrara, F. Fiorillo, L. Martino, E. Olivetti, L. Rocchino, Istituto Nazionale di Ricerca, Metrologica (INRIM), Torino, Italy

Abstract

At IBA, the steels used to build the magnets of the Cyclone230® cyclotron are cast on demand, using very strict criteria, casting procedure, requirements and quality control. Among the various steps performed at the foundry, a thermal annealing is made. In this work, we assess the usefulness of such thermal treatment.

Samples of pure iron casts have been magnetically and structurally characterized. Progressive magnetic softening was observed upon successive annealing steps. These changes of the magnetic properties were attributed to the relief of internal stresses.

Results, obtained by X-ray diffraction, electron microscope and precise determination of magnetization curve and hysteresis loop, will be presented and commented.

INTRODUCTION

The fabrication of a Cyclone230® cyclotron [1] magnet requires operations like casting, cooling, annealing, machining among others. A very good understanding of each production step and an impact of each operation on the cyclotron quality are mandatory. In addition the suppression of one operation may generate significant cost reduction leading towards more affordable system. In this case, it could make protontherapy a bit less expensive. In this context, we were encouraged to perform an extensive study of the iron casting procedure.

IBA started to collaborate with the INRIM to deploy a program of structural and magnetic studies of iron.

IRON SAMPLES



Figure 1: The selection of tested iron samples.

Tested iron samples, provided by the iron supplier, created a large variety taking into account: shape (disks,

toroids and rods), thermal treatment (unannealed, annealed at 820 C), location in the original iron casts (4 positions in the cast) and numerous samples from nearly the same position (see Fig. 1).

During analysis, some samples:

- have been ground, polished, cleaned and/or etched using a nitric acid in ethanol solution (Nital)
- have been additionally annealed in different temperatures during cycles controlled in time

MICROSTRUCTURAL INVESTIGATIONS

Grain Size

An optical microscope and a Scanning Electron Microscope (SEM) have been used to count the number of grains intercepted by arbitrary chosen sufficiently long straight lines. The number of intercepts is related to the grain size. Acquired statistics permitted to calculate the average intercept length \bar{x} and the standard deviation σ . The condition: $\sigma \geq \bar{x}$ implies large variation in observed grain size. For different samples, measurements gave values: $0.77 \text{ mm} < \bar{x} < 1.52 \text{ mm}$, $x_{max} = 8 \text{ mm}$ and $0.84 \text{ mm} < \sigma < 1.64 \text{ mm}$.

It should be noted that irregularly shaped large grains and inclusions of impurities produce multiple intersections with arbitrarily selected test lines. In this way the average intercept length and consequently the grain size are underestimated.

Some samples have been photographed in large magnification (150x) before and after thermal treatment to verify the effect of annealing on grain boundaries and to detect recrystallization or the occurrence of grain growth. From the comparisons, no changes in grain shape or grain size have been observed between unannealed state and fully annealed state of samples. The thermal treatment does not produce any recrystallization or grain growth.

Chemical Composition Of Impurities

Information on the chemical composition of the cast iron is a standard request of IBA. An example is shown in Fig. 2. The impurities content has been once again determined using a Scanning Electron Microscope (SEM) and an Energy Dispersive Spectroscopy X-ray Diffraction (EDS XRD) detector.

A high magnification (4000x) of the SEM was needed to detect different shapes and sizes of inclusions.

Unetched iron samples presented different types of inclusions like: sharp edge shapes, bar shapes, cross-shaped crystals and tree-like shapes of monocrystals or multicomponent agglomerates.

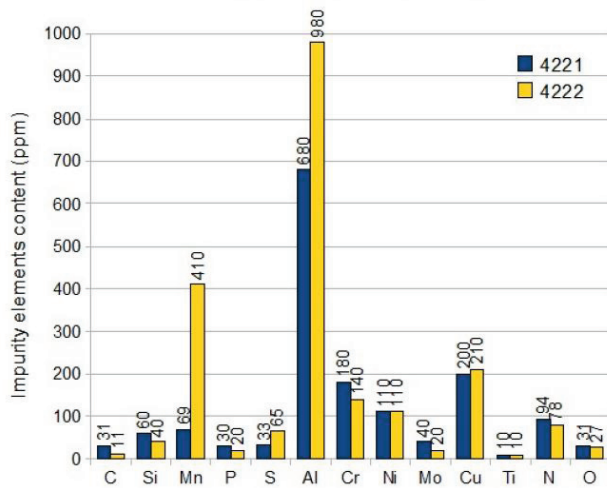


Figure 2: Impurities content in iron casts number 4221 and 4222.

The chemical etching removed the surface layer of the samples and better revealed the structure of inclusions between grain boundaries or inside grains, see Fig. 3. The surface differences and a strong hardening have been observed in the layer up to 100 μm in samples machined on the lathe.

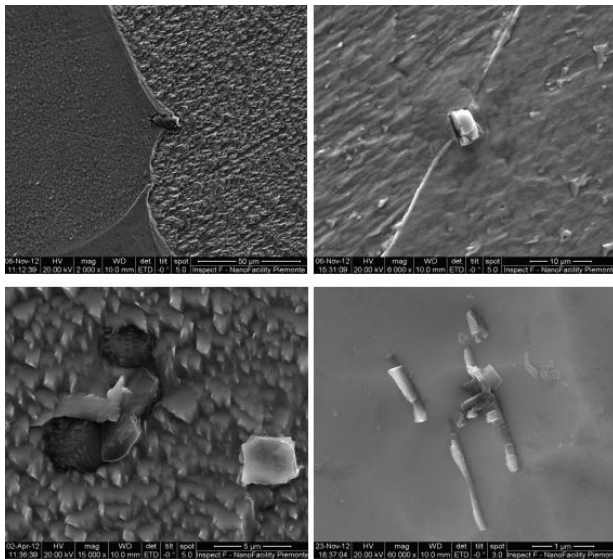


Figure 3: Example of inclusions in etched samples.

Then annealing was performed to detect possible modifications of the inclusions shape. In unetched state and after chemical etching, no differences were found with respect to shape and location of foreign crystals.

EDS XRD analysis regularly detected the presence of three chemical compounds: AlN – aluminium nitride, MnS – manganese sulphide and Al₂O₃ – aluminium oxide. The agglomerates of any two or all three compounds created a majority observed inclusions in the samples.

The chemical composition of inclusions, tested using EDS XRD detector, was also identical before and after

annealing process without any preferential directional orientation of inclusions.

Magnetic Measurements

DC magnetization curves and hysteresis loops have been measured for ring and rod iron samples. Measured data on these samples have been obtained using the point-by-point (ballistic) and the continuous hysteresisgraph methods. The hysteresisgraph method traces directly the hysteresis loop under controlled, low frequency (0.03 Hz) polarization waveform. Measurements performed on single ring iron samples extracted nearly at the same location of one cast indicated a lack of reproducibility of the hysteresis curve, see Fig. 4, where the ordinate scale presents the magnetization $J(T) = B - \mu_0 H$ instead of the usual magnetic flux induction B .

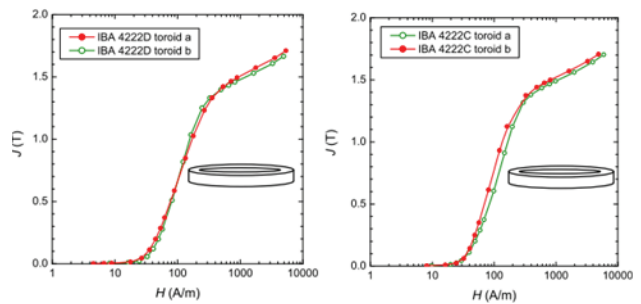


Figure 4: The lack of reproducibility of magnetization curves observed on samples from the same location in one cast.

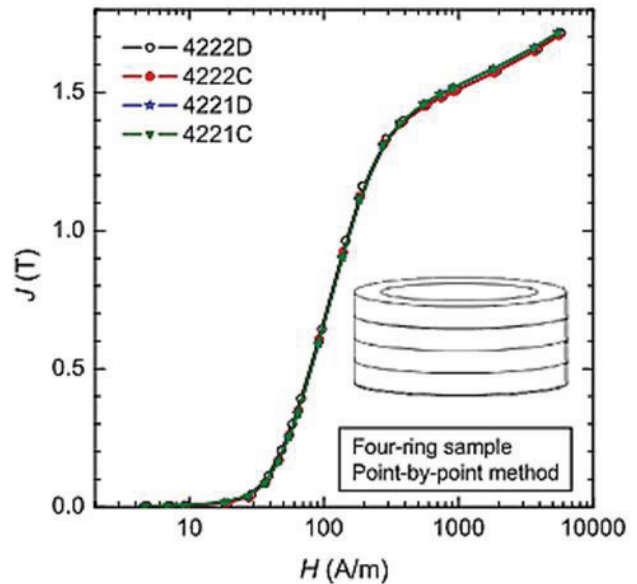


Figure 5: Magnetization curves for stacked four ring samples extracted from different casts.

The large and coarse grain structure was the reason of magnetization differences and grouping (staging) of four ring samples from a similar location in the same cast was necessary to provide reproducible results.

The magnetization differences between four ring samples taken from different iron casts are small

indicating the correct control of different casts by the iron supplier, see Fig. 5.

A closer look on details of the magnetization curves confirms a superposition of properties between casts. At the same time, details reveal the differences of energy losses (area of the hysteresis loop) up to 2% and coercive magnetic field intensity H_c between 51 and 54 A/m.

Measurements on rod samples using a permeameter also presented important differences of the hysteresis curve at different points along the rod due to coarse grain structure. The 30 mm central segment of the rod was used to average measurements of the magnetic flux and three Hall probes have been applied over this segment.

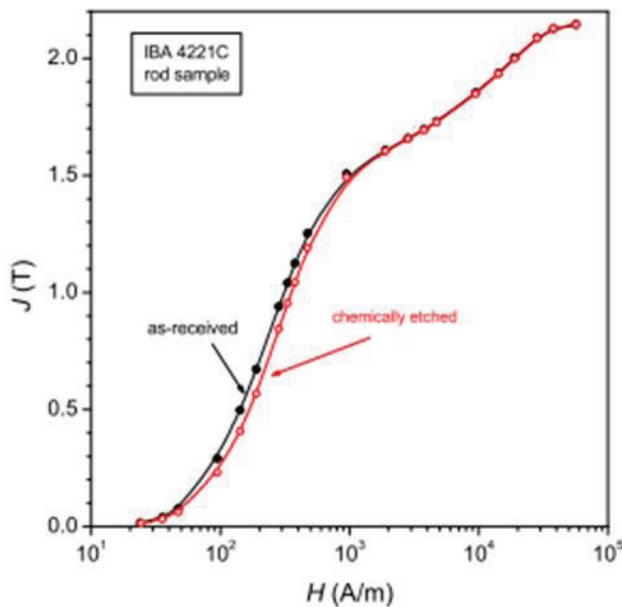


Figure 6: Magnetization curves of a rod sample tested in unannealed state, before and after chemical etching.

The magnetization curve was measured before and after chemical etching of the surface layer. A slight deterioration of the magnetic response was observed at low magnetic field intensities, Fig. 6, and was attributed to uneven surface after etching which implies local demagnetizing effects.

Magnetization curves have been measured for different annealing temperatures on different sample types and locations.

The Fig. 7 presents magnetization curves for different annealing indicating the similarity of both materials and the improvement of magnetic properties related to the annealing being a stress relief treatment. The relative magnetic permeability μ_r is improved for the magnetic fields below 1.6 T and unchanged beyond 1.6 T as one can see in Fig. 8.

This part of the measurements indicated that the thermal annealing process performed by the iron supplier has practically no effects on the iron quality.

Unfortunately, Cyclone230® cyclotron has a magnetic field induction $B > 1.75$ T in the machine centre so the advantage of correct annealing is rather small.

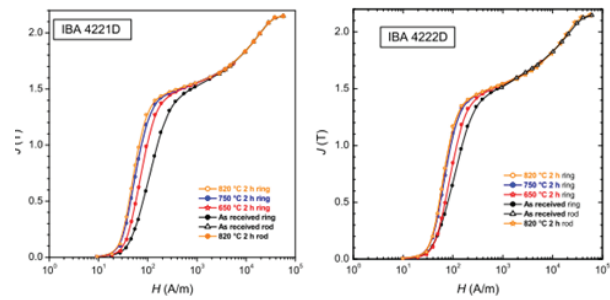


Figure 7: Magnetization curves for different annealing temperatures in samples from casts 4221D and 4222D.

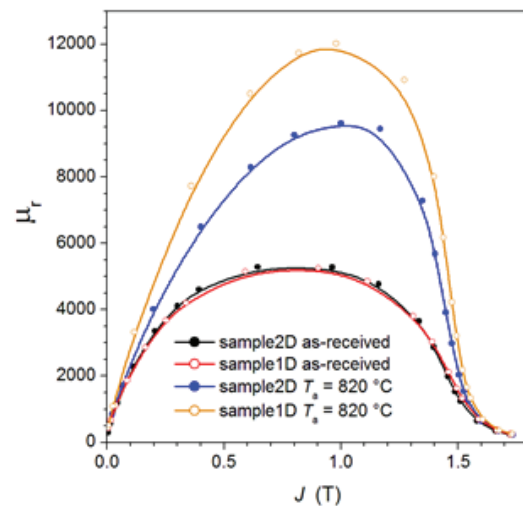


Figure 8: Increase of the relative magnetic permeability μ_r with annealing at 820 C.

CONCLUSIONS

Performed microstructural investigations and magnetic measurements indicate that the annealing performed up to date has no effects on grain size, impurities and improves the magnetic properties in less relevant region of magnetic field values. The annealing treatment of the iron cast for the Cyclone230® cyclotron can be suppressed in the future.

ACKNOWLEDGMENT

The details of measurement methods have been presented elsewhere [2].

REFERENCES

- [1] Y. Jongen et al., “Preliminary Design of a Reduced Cost Protontherapy Facility Using a Compact, High Field Isochronous Cyclotron”, Proceedings EPAC 1990, p.274-276.
- [2] E. Ferrara et al., “Microstructure and magnetic properties of pure iron for cyclotron electromagnets”, ISMANAM 2013 Conference, www.ismanam2013.it